Conformational Transitions in Model Silk Peptides

Donna Wilson, Regina Valluzzi, and David Kaplan
Department of Chemical Engineering and Biotechnology Center, Tufts University, Medford, Massachusetts 02155 USA

ABSTRACT Protein structural transitions and β-sheet formation are a common problem both in vivo and in vitro and are of critical relevance in disparate areas such as protein processing and β-amyloid and prion behavior. Silks provide a "databank" of well-characterized polymorphic sequences, acting as a window onto structural transitions. Peptides with conformationally polymorphic silk-like sequences, expected to exhibit an intractable β-sheet form, were characterized using Fourier transform infrared spectroscopy, circular dichroism, and electron diffraction. Polymorphs resembling the silk I, silk II (β-sheet), and silk III (threefold polyglycine II-like helix) crystal structures were identified for the peptide fibroin C (GAGAGS repetitive sequence). Two peptides based on silk amorphous sequences, fibroin A (GAGAGY) and fibroin V (GDVGGAGATGGS), crystallized as silk I under most conditions. Methanol treatment of fibroin A resulted in a gradual transition from silk I to silk II, with an intermediate state involving a high proportion of β-turns. Attenuated total reflectance Fourier transform infrared spectroscopy has been used to observe conformational changes as the peptides adsorb from solution onto a hydrophobic surface. Fibroin C has a β-strand structure in solution but adopts a silk I-like structure upon adsorption, which when dried on the ZnSe crystal contains silk III crystallites.

INTRODUCTION

There are numerous instances of protein polymorphic behavior. Among these are the formation of insoluble plaques from normally soluble protein in vivo, such as that of β-amyloids (De Gioia et al., 1994; Goldfarb and Brown, 1995; Goldsbury et al., 1997). Another example is the tendency of proteins in vitro to aggregate into β-conformation-rich precipitates, bypassing the protein folding process. There are also numerous instances, such as the deposition of protein on the surfaces of surgical implant materials, where adsorption of protein is accompanied by a change in conformation (Absolom et al., 1987; Lin et al., 1992). For these phenomena to be understood, model polymorphic protein sequences are needed. Proteins with simple sequences that can be crystallized as helices in each conformational polymorph would provide the ideal models from the standpoint of experimental accessibility. These features are prevalent among a class of proteins, the fibrous proteins.

Most fibrous proteins have physiological roles as protective, connective, or structural materials. Some of these self-assemble into multiphase materials, with oriented crystallites embedded in an amorphous matrix (Simmons et al., 1996; Thiel et al., 1997). Often fibrous proteins exhibit a single, dominant secondary structural motif due to their highly repetitive amino acid sequences, or have a blocky architecture, with each block giving rise to a single conformational motif. Their highly repetitive nature gives rise to very regular conformations, a feature not found in globular proteins, as well as conformations that are not usually observed in globular proteins, whose main secondary structures are the α-helix and the β-sheet (a twofold helix). Examples of helical conformations that are observed for repetitive fibrous protein sequences are the threefold polyglycine II and polyproline II helices (Andries and Walton, 1969; Crick and Rich, 1955).

Among the fibrous proteins, some silks tend to have an architecture composed of two chemically distinct repetitive motifs or "blocks": an insoluble crystallizable block and a soluble amorphous block. The crystallizable blocks comprise short-side chained, highly repetitive amino acid sequences, typically leading to the formation of antiparallel β-pleated sheets. The high glycine content of silks allows greater conformational variability than that of most proteins; thus many silks, including *Bombyx mori* silk fibroin, are polymorphic. The dominant secondary structure of silk can change, depending on the environment of the protein. While the threefold polyglycine II helix, twofold antiparallel β-pleated sheets, and a poorly characterized structure "silk I" have been observed, the conformational freedom provided by the glycine residues does not preclude other conformations, such as "intermediate helices" in the extended chain conformational region between the threefold polyglycine II conformation and the twofold β-sheet. This polymorphism, notably the ability to induce a transition from a water-soluble silk I-like form to an intractable β-sheet, provides attractive options for processing these protein materials and is probably utilized in vivo. The presence and possibility of a number of slightly different conformations and conformation selection criteria that are sensitive to the environment lead to difficulty in obtaining cross-referenced corroborating data with multiple analytical techniques.

Silk fibroin contains the repetitive hexapeptide (GAGAGS) as its consensus crystallizable sequence and (GAGAGY) as its consensus amorphous sequence (Mita et

Received for publication 7 September 1999 and in final form 18 January 2000.

Address reprint requests to Dr. David Kaplan, Department of Chemical Engineering, Tufts University, 4 Colby St., Medford, MA 02155. Tel.: 617-627-3251; Fax: 617-627-3991 E-mail: dkaplan1@emerald.tufts.edu.

0006-3495/00/05/2690/12 $2.00

al., 1994). Two crystalline polymorphs are observed for bulk silk fibroin, silk II (a β-sheet structure) and silk I, which is not well understood and may be a less extended helix than the silk II β-sheet (Ambrose et al., 1951; Fossey and Kaplan, 1994; He et al., 1999; Kratky et al., 1950; Kratky, 1956; Lotz and Cesari, 1979; Marsh et al., 1955; Valluzzi et al., 1996, 1999a; Valluzzi and Gido, 1997). Another structural polymorph observed in native silk is the silk III threefold extended helix, which forms at the air-water interface (Valluzzi et al., 1996, 1999b).

Solid-state conversion from silk I to silk II, the two polymorphs associated with bulk fibroin, has been reported (Ambrose et al., 1951; Asakura et al., 1985; Kratky, 1956; Magoshi et al., 1981; Marsh et al., 1955). This conversion has been observed using x-ray crystallographic techniques and by following the changes in the position of the conformationally sensitive amide I infrared absorption band in silk membranes before and after treatment with methanol, or by thermal induction above 180°C. Conversion of silk III to silk II due to surface pressure on a Langmuir trough has also been reported (Valluzzi et al., 1996).

To gain additional insight into these polymorphs and to show how possible conformational intermediates ("intermediate helices" between the β-strand and the polyglycine II helix) found in these fibrous proteins might be better characterized spectroscopically, two model peptides have been synthesized based on the amorphous (fibroin A) and crystallizable (fibroin C) sequences of fibroin. A third model peptide, fibroin V, was prepared as a variant of the amorphous spider dragline silk sequence and was designed to form a 12_5 helix (Table 1). The sequence of fibroin V is based on the less repetitive amorphous blocks of *Nephila clavipes* spider dragline silk (Arcidiacono et al., 1998; Beckwitt and Arcidiacono, 1994; Van Beek et al., 1999; Winkler et al., 1999). The sequence of these noncrystalline regions may be approximated by the repetitive $(G\text{-}x\text{-}y\text{-}GG\text{-}z)_n$ sequence. Recent NMR studies suggest a threefold helical conformation for the amorphous component in spider silk (Van Beek et al., 1999). Peptides with the $(GG\text{-}x)_n$ sequence have been observed in a threefold helical conformation as well (Shah et al., 1997).

MATERIALS AND METHODS

Peptide design

Three peptides were designed, mimicking different natural silk sequences. Because *B. mori* fibroin is polymorphic and possesses several different possible crystal structures and conformations, the crystallizable repeat GAGAGS was chosen as the core repetitive portion of one of the peptides, fibroin C. The serine in the hexapeptide sequence is believed to act as a "handle," directing conformation selection at a hydrophobic-hydrophilic interface through partitioning (Valluzzi and Gido, 1997; Valluzzi et al., 1999a). The amorphous blocks of fibroin also have a very simple repetitive sequence, which is similar to that found in the crystallizable blocks. The major difference between the two sequences is the presence of tyrosine rather than serine as the periodic hydrophilic residue. A peptide, fibroin A, containing a repetitive sequence, GAGAGY, was synthesized to approximate the amorphous blocks of fibroin. Fibroin A was used to explore the possible participation of the amorphous portions of the silk sequence in the silk I crystal structure. Fibroin V, a sequence based on the spider silk $(G\text{-}x\text{-}y\text{-}GG\text{-}z)_n$ repetitive sequence (x, y, and z are small to medium-sized side-chain amino acids) was also synthesized. This last peptide incorporated a pattern of hydrophobic residues that would be commensurate with a helix making five turns in 12 residues. This conformation has been suggested to model the local conformation in some random coil proteins (Hiltner et al., 1972; Ronish and Krimm, 1972; Tiffany and Krimm, 1972). In all cases, glutamic acid end blocks were added to both ends of the peptides to promote solubility (Rothwarf et al., 1996).

TABLE 1 Peptide sequences

Peptide	Amino acid sequence
Fibroin C	$(E)_5(GAGAGS)_4(E)_5$
Fibroin A	$(E)_5(GAGAGY)_4(E)_5$
Fibroin V	$(E)_5(GDVGGAGATGGS)_2(E)_5$

Peptide synthesis

Peptides were synthesized by traditional F-moc peptide synthesis and purified by high-performance liquid chromatography. The peptide compositions were confirmed by matrix-assisted laser desorption ionization, time-of-flight analysis (MALDI-TOF).

Fourier transform infrared spectroscopy

Infrared spectroscopy data were gathered in both the solid and solution states, utilizing Fourier transform infrared microscopy and an attenuated total reflectance (ATR) cell (Equinox 55; Bruker, Billerica, MA) at 4 cm^{-1} resolution. Solid-state spectra were taken for dried peptides dropped from an 18 mg/ml aqueous solution onto a ZnS crystal. This was the highest solution concentration attainable to ensure sufficient film thickness for FTIR microscopy signal detection. For peptides A and V, methanol was added to the dried peptide, and the sample was allowed to dry on the crystal surface before measurement to assess conformational changes. Solution state characterization was carried out with peptide solutions placed in a ZnSe ATR crystal cell. Spectra were taken from ~1 mg/ml aqueous solutions of the peptides at 14 reflections per measurement. ATR-FTIR experiments required lower concentrations to avoid overloading the ATR cell. Spectra were also taken after solvent evaporation.

The amide I band curves were fitted using the Peak Fit v4 (Jandel) residual peak detection and fitting procedure (Peak Fit, 1997). Baseline determination was accomplished by a linear regression analysis, data smoothing utilized the Savitsky-Golay smoothing function, and Voigt amplitude function was used to curve fit data peaks (Jansson, 1984; Langford, 1978). The Voigt amplitude function convolves a "natural" Lorentzian waveform and an independent Gaussian instrument broadening, thus producing a theoretical model for spectral lines when both types of expansion are present. The contribution of each curve to the amide I band was assessed by integrating the area under the curve and then normalizing to the total area under the amide I band.

Circular dichroism

Solution-state circular dichroism (CD) studies were performed on a Jasco J-710 Spectropolarimeter (Easton, MD). Peptides were analyzed at solution concentrations of 1 mg/ml, with a path length of 0.1 cm. CD spectra were

deconvoluted utilizing a neural network-based deconvolution program, CDNN (Bohm, 1997).

Electron diffraction

Electron diffraction data were gathered with a 200-kV JEOL 2000 Mark II Transmission Electron Microscope (Akishima, Japan) at the University of Massachusetts, Amherst MRSEC/Keck Polymer Morphology Facility. Samples were deposited on silicon monoxide and carbon-coated grids by rubbing the grids along the dried peptide surfaces of both the ZnS and ZnSe crystals.

RESULTS

Infrared data

Infrared spectra were taken for all peptides (Table 1) in both the solid and solution states. For solution-state measurements, the peptides adsorb to the hydrophobic ZnSe crystal surface with time, giving spectra of adsorbed peptide localized at the crystal-water interface. The concentration of adsorbed peptide and conformational change as a function of time were monitored. A representative peak fitting simulation has been provided (Fig. 1). No simulation had an R^2 value of less than 0.87.

Solid-state FTIR spectra

Fibroin C

The amide I band for fibroin C in the solid state shows one strong peak at 1623 cm^{-1} with a shoulder at 1647 cm^{-1}. The absorption at 1623 cm^{-1} occurs in a region that is characteristic for antiparallel β-structural frequencies (Table 2), while the absorption at 1647 cm^{-1} is usually indicative of a random coil structure (Stuart, 1997). The frequency for the random coil structure contributes less than 25% to the overall area under the amide I curve, while the area attributed to the adsorption at 1623 cm^{-1} contributes ~46%. Other minor peaks in the β-structural region (1671 cm^{-1} to 1679 cm^{-1}) contribute the remaining amide I band area. Therefore in the solid state, fibroin C primarily assumes an antiparallel β-structure (silk II).

Fibroin A and fibroin V

Solid-state absorptions in the amide I frequency region occurred at 1650 cm^{-1} (contributing 27% to the amide I band) and 1652 cm^{-1} (contributing 32% to the amide I band) for fibroin A and fibroin V, respectively. At a resolution of 4 cm^{-1} these two numbers are the same within experimental error. This vibrational frequency is observed for silk I-type structures (Dong et al., 1990; Kataoka and Uematsu, 1976; Magoshi et al., 1985; Yoshimizu and Asakura, 1990). Therefore, fibroin A and V readily adopt conformations approximating the silk I structure of silk fibroin in the solid state.

To test whether the peptides could mimic the solid-state transformation behavior of fibroin, treatment with methanol (a polar solvent) was performed for the two peptides, fibroin

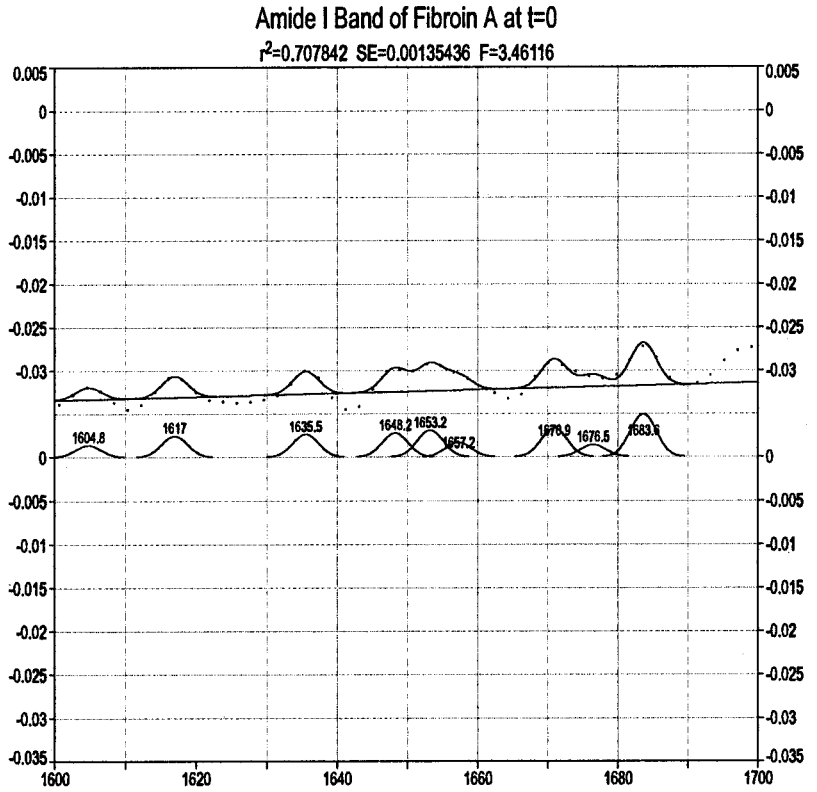

FIGURE 1 Representative peak fit analysis deriving the percentage contributions of individual peaks to the area under a curve.

TABLE 2 Characteristic secondary structural assignments for amide I band frequencies

Frequency (cm^{-1})	Secondary structure
1621–1627	β-Structure
1628–1634	β-Structure
1635–1640	β-Structure
1641–1647	Random coil
1648	Three-fold helix
1658–1666	Turns and bends
1668–1671	Turns and bends
1671–1679	β-Structure
1681–1685	Turns and bends
1687–1690	Turns and bends
1692–1696	Turns and bends

A and V, which exhibited silk I-like structures in the solid state. Treatment of fibroin A with methanol results in an incomplete conversion to the β-strand conformation (Fig. 2). An intermediate structure, characterized by a high proportion of β-turns and bends, appears. The peptide might thus exhibit these structural motifs along the conformational change pathway (e.g., silk I to silk II). Upon methanol treatment in the solid state, fibroin A exhibited strong absorptions at 1616 cm^{-1} (34%), 1633 cm^{-1} (32%), 1665 cm^{-1} (9%), 1681 cm^{-1} (13%), and 1690 cm^{-1} (9%), the region traditionally corresponding to β-structure (1616 cm^{-1} and 1633 cm^{-1}), and β-turns and bends (1665 cm^{-1}, 1681 cm^{-1}, and 1690 cm^{-1}). The strong absorption observed for untreated fibroin A at 1650 cm^{-1} decreases to less than 1% of the contribution to the amide I band after methanol treatment. While the absorption peak at 1662 cm^{-1} after methanol treatment could be assigned to a polyglycine II helix and not a β-turn for fibroin A, the characteristic amide II absorption peak at 1550 cm^{-1} for the polyglycine II helical form of poly(AGG) is absent. Instead, fibroin A shows a single absorption peak at 1515 cm^{-1} in the amide II region, which has been reported for poly(AGG) in the β-form (Abe and Krimm, 1972; Rippon and Walton, 1972).

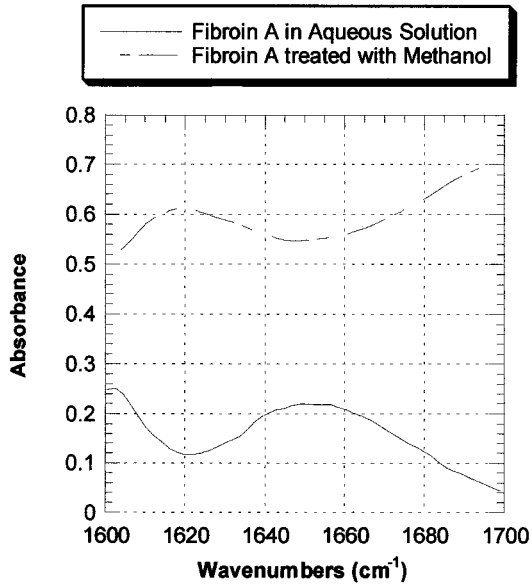

FIGURE 2 Solid-state conformational change of fibroin A observed through FTIR microscopy in the amide I region.

Conformational changes in fibroin V with methanol treatment were not as readily observed as changes in fibroin A. The appearance of a small percentage of β-structure and random coil conformations was observed after methanol treatment. However, the major absorption peak at 1652 cm^{-1} for untreated peptide persisted in the treated fibroin V, comprising ~25% of the amide I region. Strong absorptions were also observed at 1629 cm^{-1} (16%) and 1637 cm^{-1} (12%), corresponding to the β-structural region and "random coil" conformations, respectively. Additional absorptions occurred at 1662 cm^{-1} (14%) and 1671 cm^{-1} (18%) in the region associated with β-turns and bends. The 1662 cm^{-1} absorption could be interpreted as the presence of some polyglycine II or silk III conformation, which has a characteristic amide I absorbance of 1558–1663 cm^{-1}. However, similar values are cited for silk I-like structures in peptides with similar glycine-rich sequences. The strongest amide II band observed for fibroin V is at 1538 cm^{-1}, consistent with an amorphous or a silk I-type of structure.

Solution-state FTIR spectra

Solution-state conformational information was obtained using ATR-FTIR. In the initial stages of the experiments, there was negligible adsorbed peptide in the crystal, and the IR beam interrogated peptide that was primarily in the solution (in contact with or near to the crystal). As adsorption progressed, the growing adsorbed peptide layer contributed more of the spectroscopic information obtained. All of the peptides readily adsorbed to the hydrophobic surface of the ATR cell.

Fibroin C

Many peaks were observed for the solution-state structure of fibroin C, indicating that the peptide adopts a variety of ϕ and ψ angles in solution. Strong absorption peaks were observed at 1631 cm^{-1}, 1648 cm^{-1}, 1656 cm^{-1}, 1665 cm^{-1}, 1671 cm^{-1}, 1679 cm^{-1}, and 1689 cm^{-1} for fibroin C (Fig. 3 *A*). Absorptions from 1671 cm^{-1} to 1679 cm^{-1}, and 1687 cm^{-1} to 1690 cm^{-1} correspond to β-turns and bends, respectively. β-Turns and bends are expected because of the greater conformational freedom experienced by peptides in solution. Because the peptide approximates the β-structural crystalline blocks in silk fibroin, the peak at 1631 cm^{-1} is also not unexpected. However, the absorption peaks at 1656 cm^{-1} and 1665 cm^{-1} were not anticipated and change over time as more peptide adsorbs to the crystal surface (Fig. 3 *A*).

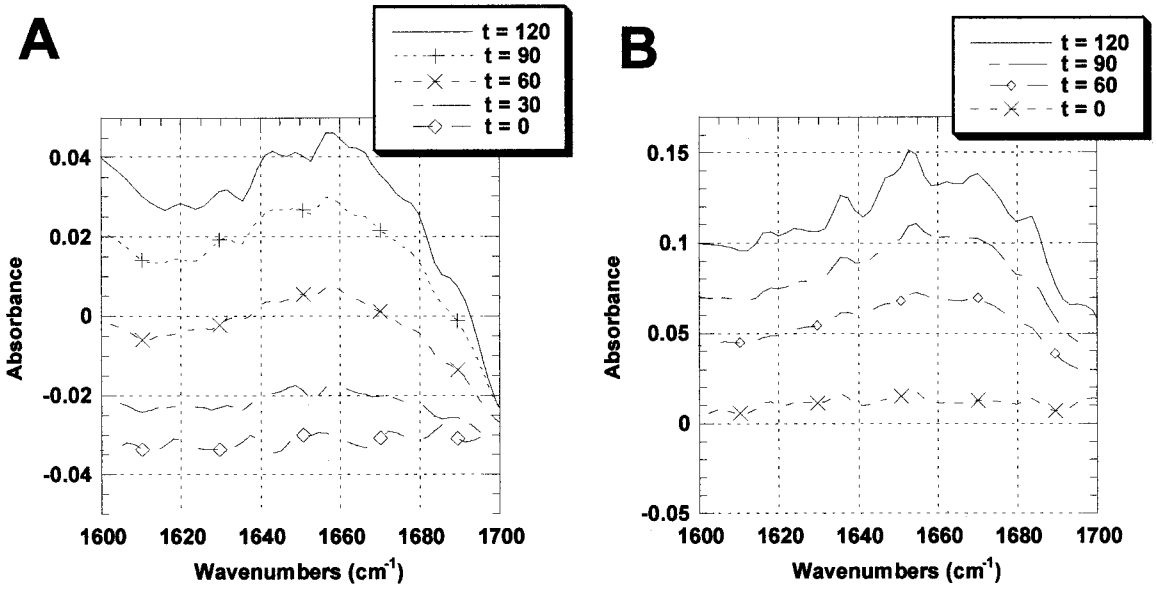

FIGURE 3 ATR-FTIR solution spectra. (*A*) Fibroin C; (*B*) fibroin A.

Poly(AGG) in its polyglycine II-like helical form (threefold helix) gives an absorption peak at 1656 cm^{-1} (amide I band) and 1550 cm^{-1} (amide II) (Rippon and Walton, 1972). Both of these peaks are present in the adsorbed fibroin C spectra. Furthermore, a peak at 1663 cm^{-1} has been observed for the polyglycine II/silk III film at the air-water interface (unpublished data), and Abe and Krimm calculated the vibrational frequency for the threefold polyglycine II helix at 1648 cm^{-1} with an observed frequency of 1654 cm^{-1} (Abe and Krimm, 1972). Thus elements of threefold helical conformation may be present in addition to the β-strand conformation or may occur in the initial adsorbed peptide layer.

Fibroin A and V

The FTIR-ATR spectra for fibroin A and V also showed more than one absorption peak in the amide I region, indicating conformational variability in solution. However, the absorption peaks did not change their contribution to the amide I band with time (adsorbed film thickness), as was the case for fibroin C (Fig. 3 *A*). The highest infrared absorption intensities occurred at 1636 cm^{-1}, 1646 cm^{-1}, 1653 cm^{-1}, 1660 cm^{-1}, and 1670 cm^{-} for both peptides (Fig. 3 *B*; fibroin V not shown). The peaks at 1646 cm^{-1} and 1653 cm^{-1} are characteristic of silk I vibrational frequencies and are not surprising because fibroin A and V are designed to reproduce the silk I form of fibroin. The 1660 cm^{-1} and 1670 cm^{-1} amide I peaks probably correspond to β-turns and bends, rather than to threefold extended helical structures, because the infrared amide II absorption at 1550 cm^{-1} characteristic for polyglycine II is absent. As with fibroin C, turns and bends would be expected for the peptides in solution because of the greater conformational freedom of the ϕ and ψ angles in solution.

Time-dependent changes for solution state

Fibroin A and V

The relative contributions of the different components of the amide I band deviate less than ~2% over a 100-min adsorption experiment (Fig. 4). The rate of peptide adsorption to the crystal surface is linear, with the final concentration of peptide solution above the surface reaching 0.568 mg/ml after 2 h (Fig. 5). The rate of adsorption is ~0.3 mg/ml/h from a starting concentration of ~1.0 mg/ml.

Fibroin C

The solution-state spectra for the adsorbed fibroin C show an absorption peak at 1631 cm^{-1}, $t = 0$, that decreases with time from ~10% to 0%, indicating a decrease in β-structure with increased peptide adsorption to the surface of the ATR cell (Fig. 6). The peaks at 1648 cm^{-1} and 1665 cm^{-1} increase in contribution to the amide I band with time. The absorption at 1648 cm^{-1} begins with an approximate 8% contribution and increases to 17%, while the 1665 cm^{-1} peak begins at 5% and increases to 17%. The peak at 1656 cm^{-1} remains constant in percentage contribution to the amide I band throughout the experiment. The rate of peptide adsorption to the crystal surface is linear, with the final concentration of peptide solution above the surface at 0.727 mg/ml after 2 h (Fig. 5). The rate of adsorption is ~0.3 mg/ml/h from a starting concentration of ~1.0 mg/ml, the same as that found for fibroin A and V.

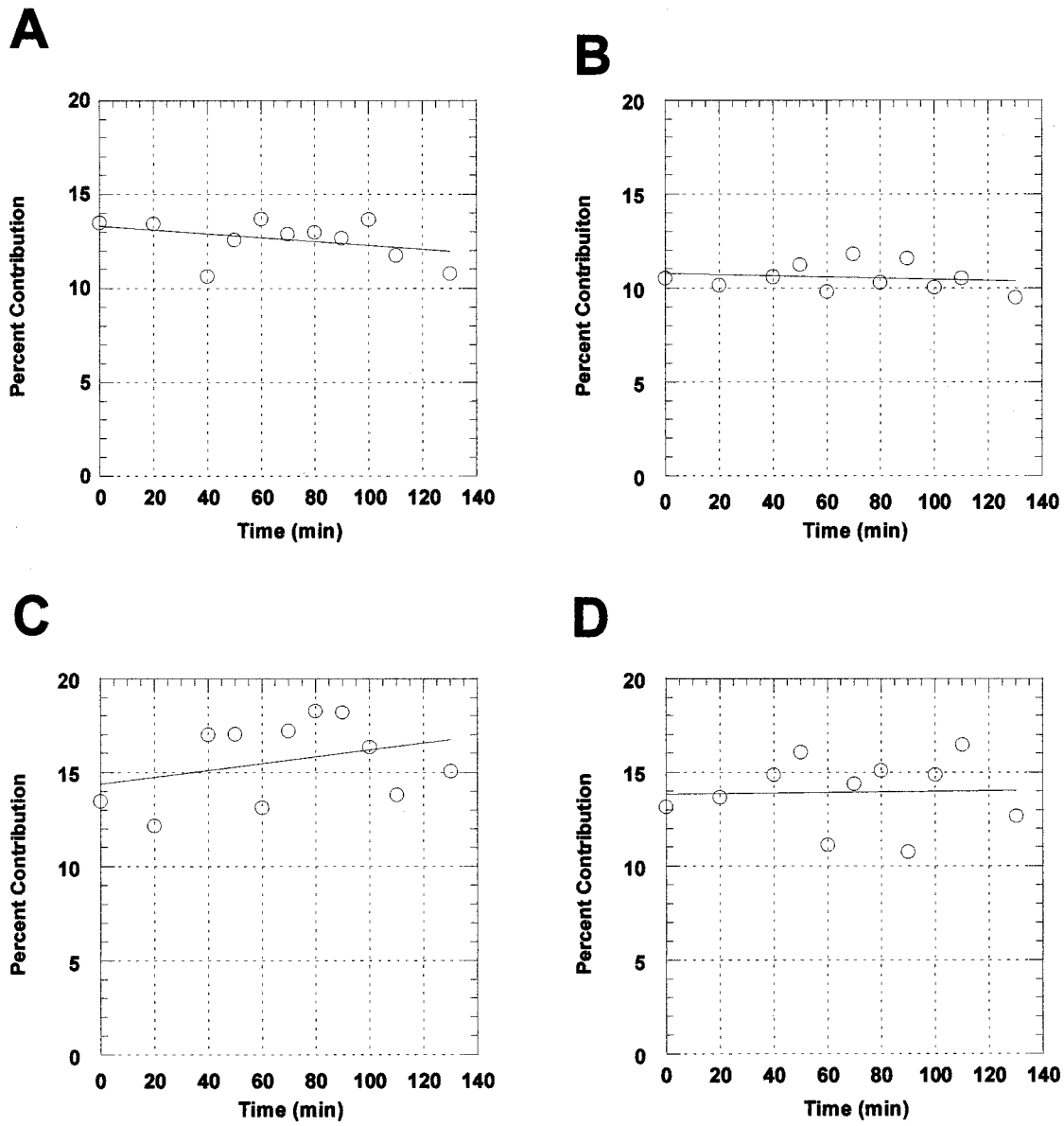

FIGURE 4 Plots of percentage contributions of various frequencies to the amide I band of fibroin A (not all peaks shown) as a function of time. (*A*) 1636 cm^{-1}; (*B*) 1646 cm^{-1}; (*C*) 1653 cm^{-1}; (*D*) 1660 cm^{-1}.

Unlike fibroin A and V, which are silk I-like in solution, when fibroin C adsorbs to a hydrophobic surface its conformation is altered, as evidenced by changes in the relative contributions of the different components of the amide I band (conformations). Fibroin C undergoes changes in conformation when it adsorbs to the hydrophobic ZnSe surface: from the β-structure to a more compressed helix, similar to silk I, or possibly a threefold polyglycine II-like structure. Further studies will help to determine whether the conformational change is due to the hydrophobic nature of the substrate or to peptide localization at the crystal-water interface. Because the sequence of fibroin C differs from $(G)_n$, slight deviations in the absorption intensities would be expected. However, the slight change in primary sequence substitution of alanine for glycine in every other amino acid can be accommodated in this helix without significant distortion. Assignment of specific helical conformations to the silk I-like and polyglycine II-like spectra is not possible with the current available data—further corroboration through crystallographic techniques is needed.

Circular dichroism

CD spectra were taken for all peptides in water free of salts. Traditional deconvolution programs do not provide good

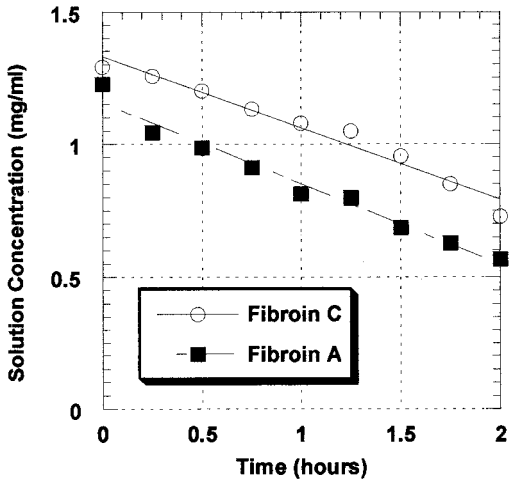

FIGURE 5 Rates of adsorption of fibroin C and fibroin A onto the hydrophobic ZnSe crystal surface.

approximations of the secondary structure of fibrous proteins/peptides because globular protein databases are used to compare CD spectra. Therefore, the conclusions drawn by the deconvolution of the spectra can only be interpreted as rough approximations until better databases based on fibrous protein structures are available. However, deconvolution of CD spectra for fibroin C indicated more β-structure than for fibroin A and fibroin V by $>6.05\%$ and $>10.15\%$, respectively.

The CD absorption spectrum for fibroin V closely approximates a non-β-strand extended helical structure with a curve minimum at 197 nm and $-20\theta \times 180\times 10^{-3}$ and a maximum at $\sim$215 nm and $+5.0\theta \times 180\times 10^{-3}$ (Rippon and Walton, 1971; Ronish and Krimm, 1974; Tiffany and Krimm, 1972). Polypeptides that form extended helical structures, such as poly(AGG), poly-L-aspartic acid, and poly-L-proline, tend to have curve minima at $\sim$198 nm and maxima at 213–218 nm. Furthermore, the characteristic minima for unordered polypeptide chains in the 210–220-nm region are absent from the fibroin V CD spectra, suggesting an extended helical structure for fibroin V (Ronish and Krimm, 1972).

Electron diffraction

Electron diffraction data were obtained for fibroin C under a number of different conditions. Preliminary results from lyophilized fibroin C were obtained in the TEM without further sample preparation, and an amorphous structure was observed, exhibiting a single diffuse diffraction ring centered at 4.5 Å. Initial data were also obtained by wiping the ZnS crystal with a TEM grid to pick up solid material from the film used for FTIR. These samples were found to have a silk II-like antiparallel β-sheet structure with characteristic reflections at 4.6 Å and 4.7 Å, corresponding to the interchain and intersheet spacings observed for β-sheets of silk (Fraser et al., 1966; Lotz and Cesari, 1979; Magoshi et al., 1985; Takahashi, 1994). This observation corroborates the solid-state FTIR spectra obtained for fibroin C. An aqueous solution of fibroin C at room temperature was dropped onto amorphous carbon films for TEM and allowed to dry (amorphous carbon is very hydrophobic). Samples prepared in this way exhibited crystal structures markedly similar to the silk III structure observed for native silk at the air-water interfaces (Valluzzi et al., 1996, 1999b; Valluzzi and Gido, 1997). Hexagonal patterns of single crystal diffraction spots were observed at 4.6 Å. Pairs of diffracted spots were also observed at 3.2 Å and 18.6 Å, corresponding to the rise per residue (the 006 reflection), and the chain axis spacing for sixsidues (the 001 reflection), respectively. Characteristic reflections for silk III at 4.66, 5.15, and 5.44 Å were also observed (Valluzzi and Gido, 1997). Thus the sample preparation conditions, especially the properties of the solid surface used to prepare films, affect the conformational and crystalline polymorph obtained for fibroin C.

To corroborate the ATR-FTIR observations, TEM samples of fibroin C were obtained at two points during the ATR-FTIR experiments. When material was taken from the adsorbed peptide at the ZnSe crystal-water interface, electron diffraction data indicated an amorphous or poorly crystalline silk I-like structure. When the adsorbed peptide was allowed to dry as a thin film in the ATR cell, characteristic reflections for silk III were observed. In both cases material was obtained by wiping a hydrophobic carbon-substrate TEM grid across the surface of the film to pick up material. For wet and soft samples, the use of a hydrophobic carbon substrate immobilizes the structure and prevents further crystallization and spreading. Morphologies of the silk I-like peptides from TEM images are provided in Fig. 7.

DISCUSSION

The development of secondary structure is an important consideration in protein folding and in the hierarchical self-assembly of ordered protein domains. Fibrous proteins, unlike globular proteins, contain repetitive amino acid sequences, giving rise to very regular secondary protein structures. In addition, fibrous proteins in many cases exhibit α-helical and/or β-sheet conformations, but also can assume other conformations not observed in globular proteins, such as the β-spiral and polyglycine II helix. Because these conformations are not well represented in standard spectroscopic data sets, they are difficult to infer from a typical spectroscopic characterization of secondary structure. The predominant helical conformation adopted by the repetitive sequences in fibrous proteins can incorporate most of the protein molecule such that fibrous proteins tend to exhibit one dominant structure. Therefore, it may be possible to identify spectroscopic trends that distinguish more of the subtleties of these conformations and to examine intercon-

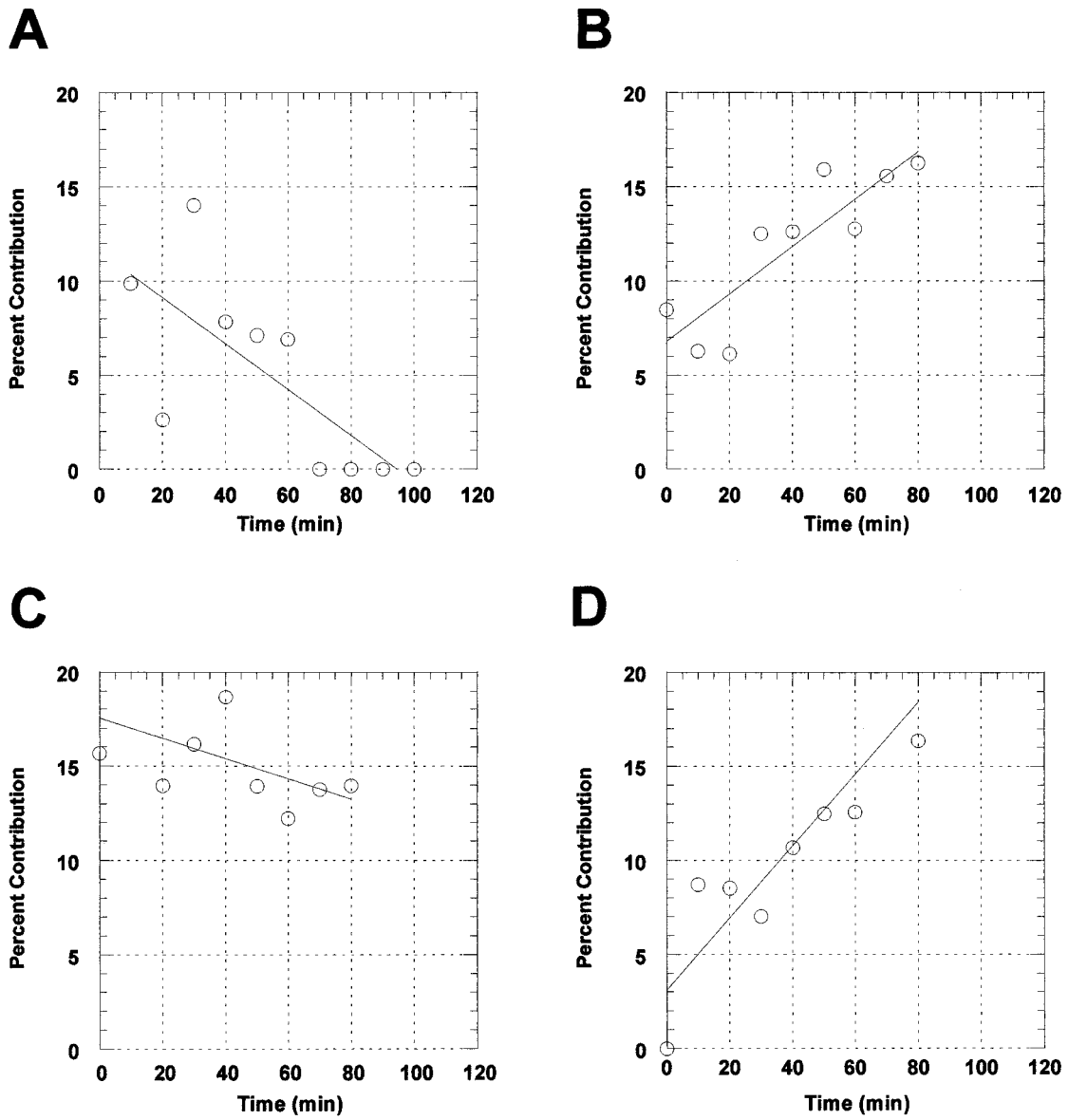

FIGURE 6 Plots of percentage contributions of the various frequencies to the amide I band of fibroin C (not all peaks shown) as a function of time. (*A*) 1631 cm^{-1}; (*B*) 1648 cm^{-1}; (*C*) 1656 cm^{-1}; (*D*) 1665 cm^{-1}.

version of these conformations to determine how it might occur. These results may also provide insights into conformational transition and folding pathways in globular proteins.

In both the solution state and the solid state, the structural polymorphism observed for the peptides depends on sequence pattern. The sequences are identical in length and contain the same proportion of glycine residues, a factor that has previously been observed to contribute to conformation selection in polypeptides (Abe and Krimm, 1972; Rippon and Walton, 1972). The patterns of hydrophilic and hydrophobic residues and of larger and smaller residues presented by the peptide sequences are different. Fibroin C is the only one of the three model peptides that preserves the six-residue hydrophilic and hydrophobic periodicity of the native silk crystallizable sequence (GAGAGS) without substituting in larger, conformation-limiting residues (tyrosine in fibroin A). Thus it is not surprising that similar conformational templating behavior is observed for fibroin C at a hydrophobic interface, as is seen for native fibroin, but is absent in fibroin A and V, which simulate amorphous or random coil-generating sequences. The behavior observed upon substitution of tyrosine for serine (when comparing the sequences of fibroin A, fibroin C, and native fibroin) suggest that amorphous tyrosine-containing blocks of the native sequence do not play a crucial role in selection of the silk I, II, and III polymorphs.

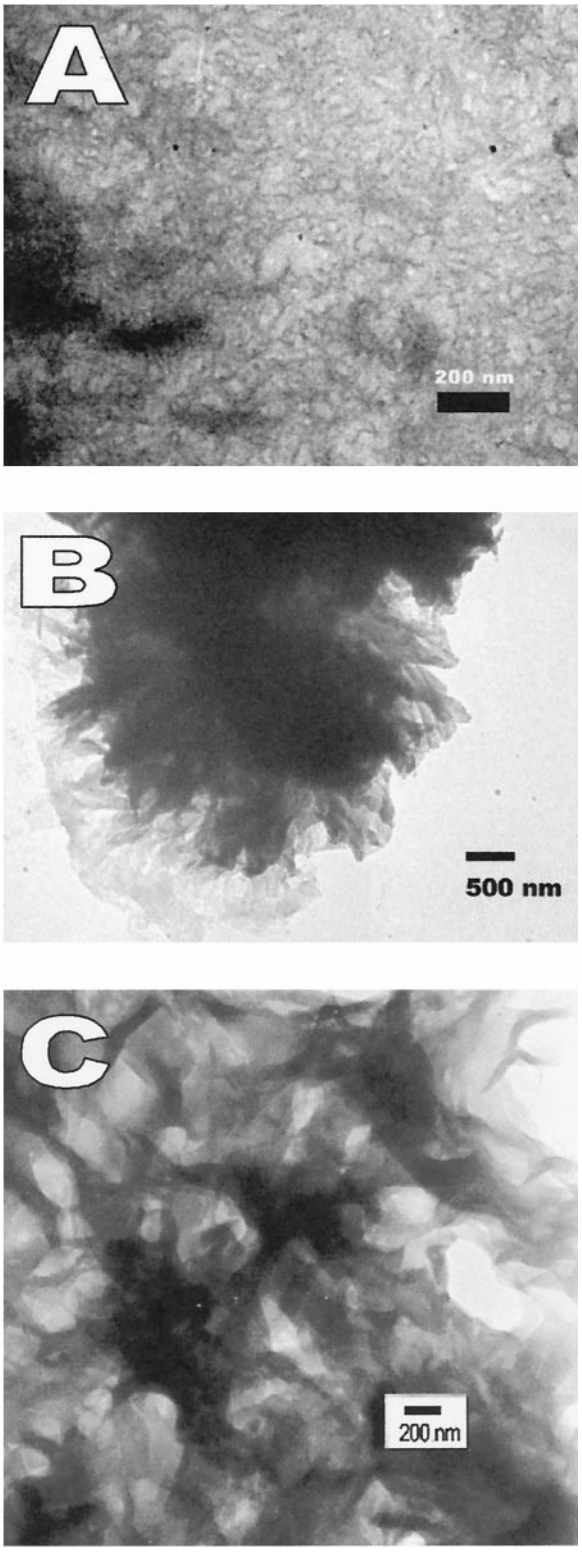

FIGURE 7 Reticulated morphologies observed by TEM for silk I-like peptides. (*A*) Fibrous film formed by fibroin A. (*B*) Precipitate from fibroin A with reticulated structures visible on the perimeter of the precipitate. (*C*) Reticulated fibrous film formed by fibroin V.

Small modifications in the repetitive sequence can have a noticeable effect on the behavior of the peptides. Fibroin A and fibroin C have identical hydrophilic/hydrophobic periodicities, but fibroin C is composed of only small residues and can adopt the largest number of conformational polymorphs. The solution-state conformations, solid-state structures, and adsorption behavior for the two peptides are quite different, even though their repetitive sequences differ by only one residue. Similarly, fibroin V has a repetitive sequence that is 50% glycine and is rich in (G-G-x) motifs, but this peptide does not readily form β-strand or β-sheet structures. In studies of silk-like polypeptides, sequences composed of the (G-x), (G-G-x), and (G-G-G-x) motif could all be readily obtained in a β-sheet crystalline polymorph, as can many polypeptides modeling fibrous proteins (Fraser et al., 1965, 1966; Kataoka, 1977; Keith et al., 1969; Komatsu, 1985; Lotz and Cesari, 1979). The difference between fibroin V and the similar β-sheet-forming sequence is not a difference in amino acid composition, but rather a modification in amino acid pattern.

The effect of hydrophobic and hydrophilic sequence patterning on preferred protein conformation has been noted previously. In a study where sequences were designed with the same amino acid composition but with different patterning of hydrophobic residues, peptides adopted polar conformations upon adsorption from an aqueous (hydrophilic) liquid to a hydrophobic surface (DeGrado and Lear, 1985). The hydrophobic residue periodicity determined the conformation adopted, with hydrophobic residues aligning themselves with the hydrophobic surface and the hydrophilic residues interacting with the solvent.

The pattern of hydrophobic and hydrophilic residues in the peptide repetitive sequences clearly affects the nature of the conformations adopted by the peptides and the possibility of structural transitions. This effect is notable in the adsorption studies. None of the peptide sequences have a periodic pattern of hydrophobic and hydrophilic residues that would help stabilize a β-strand conformation at a hydrophobic/hydrophilic interface. In fact, all three peptides were designed with sequences that would favor alternative extended coil conformations at such an interface. The two "amorphous sequence" peptides, fibroin A and fibroin V, adsorbed to the hydrophobic interface with essentially no change in conformation. Fibroin C underwent a structural change upon adsorption to adopt a conformation more closely mimicking the silk I conformation favored by fibroin A, and upon drying selected a conformation that separates hydrophobic and hydrophilic residues to opposite sides of the interface.

Conformational changes upon adsorption to a hydrophobic interface are not unexpected and have been observed to involve partitioning of hydrophobic and hydrophilic residues. While the effects of an interface on protein structure and conformation are often neglected in studies of protein conformation, especially ATR-FTIR spectroscopic analy-

ses, such effects are widespread and are well known (Bauer et al., 1994; Caessens et al., 1999; Feng and Andrade, 1994; Loeb and Baier, 1968; Malcolm, 1962, 1970a; Maste et al., 1997). Interfacial denaturation and conformational changes have been studied for a large number of proteins. In most cases, the effect of a hydrophilic interface is less pronounced than that of a hydrophobic interface (Buijs and Hlady, 1997; Matsuno et al., 1991; Norde and Zoungrana, 1998; Wu et al., 1993). The conformational diversity observed for fibroin C and the dependence of conformation on the solid substrate (against which an aqueous solution is dried) indicate that the interaction between the peptide and the solid surface is one mechanism that can drive the selection of conformational polymorphs. Similar effects have been noted in studies of globular proteins adsorbed to hydrophobic surfaces, where the protein adopts a random coil-rich conformation in the early stages of adsorption, followed by the appearance of secondary structural elements as the amount of protein in the adsorbed layer increases (Bauer et al., 1994; Wu et al., 1993). The relative proportions of the different secondary structures observed in the adsorbed layer are different from those observed for the protein in solution; there is a conformational change (Biridi, 1973; Castelain and Genot, 1994; Dufour et al., 1998; Malcolm, 1968, 1970b; Narsimhan and Uraizee, 1992; Smith and Clark, 1992). As an example of this behavior in a fibrous protein, a conformational change has been observed for native silk fibroin at the air-water interface, where air provides an essentially hard, very hydrophobic interface (Valluzzi et al., 1996, 1999a,b; Valluzzi and Gido, 1997).

The solution-state structures observed for the peptides and the structures observed for peptides precipitated from solution contrast with the structures obtained by adsorption to an interface. The conformations selected by each peptide upon adsorption to a hydrophobic interface appear to be strongly driven by the hydrophobic periodicity inherent in each repetitive residue pattern. The factors driving solution-state conformation selection are less readily apparent. Fibroin C and fibroin A have very similar repetitive hexapeptide sequences, with a hydrophilic residue occurring periodically at every sixth position in the sequence. In the FTIR-ATR adsorption experiment, these sequence similarities led to similar conformations on a hydrophobic surface. In addition, both peptides can be obtained in the β-sheet structural polymorph in the solid state. However, the solution-state conformations favored by these two sequences are very different; fibroin A adopts a random coil/silk I-like conformation, while fibroin C adopts a β-sheet conformation.

For isolated molecules in solution, sterical considerations that would exist in a β-sheet crystal structure are relaxed. For example, factors leading to constant-density β-sheets without significant deformation, such as the relative sizes of side chains in the β-sheet intersheet region and whether or not the pattern of residues permits interdigitation, are not expected to be of crucial importance for the stability of an isolated β-strand. Similarly, without a hydrophobic interface to partition hydrophobic and hydrophilic residues, the thermodynamic driving force for such partitioning of residues in isolated molecules in solution is not evident. The solution conformation of fibroin V is especially notable in this respect; circular dichroism indicates a nonrandom coil structure for fibroin V in solution, very similar to the "approximately threefold" and 12_5 helical conformations proposed to explain CD results for similar polypeptides (Rippon and Walton, 1971, 1972; Ronish and Krimm, 1972; Tiffany and Krimm, 1972). The solution-state conformations adopted by the peptides could be rationalized if they cluster or interact in solution, although the nature of this possible interaction remains unknown at this time. Similar tendencies in solution-state conformations adopted by peptides, which are also possible to rationalize if the peptides interact, were observed by DeGrado and Lear (1985).

The relationship between peptide sequence and the mechanism of solid-state transformation from a silk I-like structure to a β-sheet structure requires further elucidation at this time. While β-turn-rich intermediates are observed during solid-state transformation of fibroin A to a β-sheet form, it cannot be demonstrated from these results whether or not the ability of the peptide sequence to form such intermediate structures is a necessary prerequisite for a solid-state transformation to a β-structure. Fibroin V does not show a similar solid-state transformation and has not been obtained as a β-sheet structure. Structures involving a high proportion of turns are not observed for this peptide when it is treated with methanol. However, because the β-sheet structure is evidently not favorable for fibroin V, it is unclear whether the lack of a solid-state transition for this peptide is due the intermediate structure being unfavorable, or to the unfavorable nature of the final structure (the β-sheet). In a β-strand conformation, the fibroin V sequence mixes hydrophobic and hydrophilic residues on each side of the strand, which would lead to mixing of these residues along the surfaces of a β-sheet. Furthermore, large and small residues are also mixed, and the pattern of large and small residues presented in a β-strand conformation precludes interdigitation of residues to create a uniform-density β-sheet structure (without local deformations in the sheet).

One interesting development arising from the ATR-FTIR experiments is that the silk I structure seems to be an intermediate between the silk II β-strand and the silk III structure. In solution, fibroin C exists as a β-strand. Upon adsorption to the ATR cell, the FTIR spectra for fibroin C shift toward spectra observed for silk I. Crystallographic experiments also indicate a silk I-like structure for samples obtained at this hydrophobic/hydrophilic crystal-water interface. After the peptide had dried against the crystal, FTIR and diffraction data indicate a silk III-like structure.

The FTIR data shown here, corroborated by electron diffraction, show that spectroscopic structural characteriza-

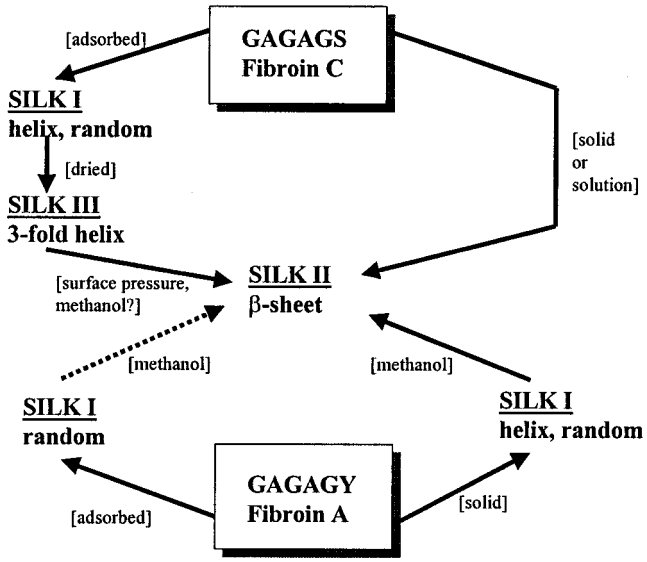

FIGURE 8 Summary of structural conformations observed for fibroin C, A, and V.

tion of these fibrous structures, as well as intermediate conformations of helices, can be cataloged and quantified. Furthermore, the conformational transitions of the peptides can be monitored, allowing insight into intermediate structures that may be adopted along the "folding" pathway and the conditions under which these structural transformations are observed (Fig. 8). Of particular interest is the observation that a β-structure can adopt an alternative extended helical structure upon adsorption to a hydrophobic surface. Other coatings for the ATR cell, of varying hydrophobicity, are being investigated to further understand this phenomenon. Additional structural peptides that might behave in the same manner are being investigated as well. These insights have important implications for assembled protein-based materials and help to elucidate the natural precursors involved in fibrous protein assembly, such as in silk spinning, collagen assembly, and the polymorphic precursors in β-amyloid disease (McGrath and Kaplan, 1997).

Discussions with Shu-Jun Chen, Shi-Juang He, Thieu Vuong, and Sam Gido (U Mass, Amherst), Edward T. Atkins (University of Bristol, UK), and Jun Magoshi (Japanese Agricultural Research Institute, Japan) are gratefully acknowledged.

Support from the National Science Foundation (NSF) (BES-9727401, DMR-970862), the NSF MRSEC program, the W. M. Keck Foundation Laboratory for Biomimetic Materials Characterization (Tufts), and the Polymer Morphology Laboratories and MRSEC facilities (U Mass, Amherst) is also gratefully acknowledged.

REFERENCES

Abe, Y., and S. Krimm. 1972. Normal vibrations of polyglycine II. *Biopolymers.* 11:1841–1853.

Absolom, D. R., W. Zingg, and A. W. Neumann. 1987. Protein adsorption to polymer particles: role of surface properties. *J. Biomed. Mater. Res.* 21:161–171.

Ambrose, E. J., C. H. Bamford, A. Eliiott, and W. E. Hanby. 1951. Water-soluble silk: an α-protein. *Nature.* 167:264–265.

Andries, J. C., and A. G. Walton. 1969. Morphological evidence for the folding of polyproline II helices. *Biopolymers.* 8:523–529.

Arcidiacono, S. A., C. Mello, D. Kaplan, S. Cheley, and H. Bayley. 1998. Expression, purification and characterization of recombinant spider dragline silk. *Appl. Microbiol. Biotechnol.* 49:31–38.

Asakura, T., A. Kuzuhara, R. Tabeta, and H. Saito. 1985. Conformation characterization of *Bombyx mori* silk fibroin in the solid state by high-frequency ^{13}C cross polarization-magic angle spinning NMR, x-ray diffraction, and infrared spectroscopy. *Macromolecules.* 18:1841–1845.

Bauer, H. H., M. Muller, J. Goette, H. P. Merkle, and U. P. Fringeli. 1994. Interfacial adsorption and aggregation associated changes in secondary structure of human calcitonin monitored by ATR-FTIR spectroscopy. *Biochemistry.* 33:12276–82.

Beckwitt, R., and S. Arcidiacono. 1994. Sequence conservation in the C-terminal region of spider silk proteins (Spidroin) from *Nephila clavipes* (Tetragnathidae) and *Araneus bicentenarius* (Araneidae). *J. Biol. Chem.* 269:6661–6663.

Biridi, K. S. 1973. Spread monolayer films of proteins at the air-water interface. *J. Colloid Interface Sci.* 43:545–547.

Bohm, G. 1997. CD Spectra Deconvolution. Delphi, Halle.

Buijs, J., and V. Hlady. 1997. Adsorption kinetics, conformation, and mobility of the growth hormone and lysozyme on solid surfaces, studied with TIRF. *J. Colloid Interface Sci.* 190:171–81.

Caessens, P. W., H. H. De Jongh, W. Norde, and H. Gruppen. 1999. The adsorption-induced secondary structure of beta-casein and of distinct parts of its sequence in relation to foam and emulsion properties. *Biochim. Biophys. Acta.* 1430:73–83.

Castelain, C., and C. Genot. 1994. Conformational changes of bovine serum albumin upon its adsorption in dodecane-in-water emulsions as revealed by front-face steady-state fluorescence. *Biochim. Biophys. Acta.* 1199:59–64.

Crick, A., and F. H. C. Rich. 1955. Structure of polyglycine II. *Nature.* 176:780–781.

De Gioia, L., C. Selvaggini, E. Ghibaudi, L. Diomede, O. Bugiani, G. Forloni, F. Tagliavini, and M. Salmona. 1994. Conformational polymorphism of the amyloidogenic and neurotoxic peptide homologous to residues 106–126 of the prion protein. *J. Biol. Chem.* 269:7859–7862.

DeGrado, W. F., and J. D. Lear. 1985. Induction of peptide conformation at apolar/water interfaces. 1. A study with model peptides of defined hydrophobic periodicity. *J. Am. Chem. Soc.* 107:7684–7689.

Dong, A., P. Huang, and W. S. Caughey. 1990. Protein secondary structures in water from second-derivative amide I infrared spectra. *Biochemistry.* 29:3303–3308.

Dufour, E., M. Dalgalarrondo, and L. Adam. 1998. Conformation of beta-lactoglobulin at an oil/water interface as determined from proteolysis and spectroscopic methods. *J. Colloid Interface Sci.* 207:264–272.

Feng, L., and J. D. Andrade. 1994. Protein adsorption on low-temperature isotropic carbon. I. Protein conformational change probed by differential scanning calorimetry. *J. Biomed. Mater. Res.* 28:735–743.

Fossey, S. A., and D. L. Kaplan. 1994. Molecular modeling studies on silk peptides. *In* Silk Polymers: Materials Science and Technology. D. L. Kaplan, W. W. Adams, B. Farmer, and C. Viney, editors. American Chemical Society, New York. 1529–1541.

Fraser, R. D. B., T. P. MacRae, and F. H. C. Stewart. 1966. Poly-L-alanylglyl-L-alanylglycyl-L-serylglycine: a model for the crystalline regions of silk fibroin. *J. Mol. Biol.* 19:580–582.

Fraser, R. D. B., T. P. MacRae, F. H. C. Stewart, and E. Suzuki. 1965. Poly-L-alanylglycine. *J. Mol. Biol.* 11:706–712.

Goldfarb, L. G., and P. Brown. 1995. The transmissible spongiform encephalopathies. *Annu. Rev. Med.* 46:57–65.

Goldsbury, C. S., G. J. Cooper, K. N. Goldie, S. A. Muller, E. L. Saafi, W. T. Gruijters, M. P. Misur, A. Engel, U. Aebi, and J. Kistler. 1997.

Polymorphic fibrillar assembly of human amylin. *J. Struct. Biol.* 119: 17–27.

He, S.-J., R. Valluzzi, and S. P. Gido. 1999. Silk I structure in *Bombyx mori* silk foams. *Int. J. Biol. Macromol.* 24:187–195.

Hiltner, W. A., A. J. Hopfinger, and A. G. Walton. 1972. Helix-coil controversy for polyamino acids. *J. Am. Chem. Soc.* 94:4325–4327.

Jansson, P. 1984. Applications in Spectroscopy. Academic Press, San Diego.

Kataoka, K. 1977. On the amorphous to beta transition of silk sericin. *Kobunshi Robunshu Eng. Ed.* 6:1–9.

Kataoka, K., and I. Uematsu. 1976. On the random coil → alpha-form transition of silk fibroin. *Kobunshi Ronbunshu Eng. Ed.* 5:620–634.

Keith, H. D., F. J. Padden, Jr., and G. Giannoni. 1969. Crystal structures of β-poly-L-glutamic acid and its alkaline earth salts. *J. Mol. Biol.* 43: 423–438.

Komatsu, K. 1985. Chemical and structural studies on silk. *In* The 7th International Wool and Textile Research Conference, Tokyo.

Kratky, O. 1956. Zur Molekularen Morphologie des Seidenfibroins. *Mh. Chem.* 87:269–280.

Kratky, O., E. Schauenstein, and A. Sekora. 1950. An unstable lattice in silk fibroin. *Nature.* 165:319–320.

Langford, J. I. 1978. A rapid method for analysing the breadths of diffraction and spectral lines using the Voigt function. *J. Appl. Crystallogr.* 11:10–14.

Lin, Y. S., V. Hlady, and J. Janatova. 1992. Adsorption of complement proteins on surfaces with a hydrophobicity gradient. *Biomaterials.* 13: 497–504.

Loeb, G. I., and R. E. Baier. 1968. Spectroscopic analysis of polypeptide conformation in polymethyl glutamate monolayers. *J. Colloid Interface Sci.* 27:38–45.

Lotz, B., and C. Cesari. 1979. The chemical structure and the crystalline structures of *Bombyx mori* silk fibroin. *Biochimie.* 61:205–214.

Magoshi, J., S. Kamiyama, and S. Nakamura. 1985. Crystallization of silk fibroin induced under various conditions. *In* 7th International Wool Textile Research Conference, Tokyo. 337.

Magoshi, J., Y. Magoshi, and S. Nakamura. 1981. Physical properties and structure of silk. VII. Crystallization of amorphous silk fibroin induced by immersion in methanol. *J. Polym. Sci. Polym. Phys. Ed.* 19:185–186.

Malcolm, B. R. 1962. Conformation of synthetic polypeptides and protein monolayers at interfaces. *Nature.* 4195:901–902.

Malcolm, B. R. 1968. Multilayer formation by a compressed monolayer of poly-epsilon-benzyloxycarbonyl-L-lysine. *Biochem. J.* 110:733–737.

Malcolm, B. R. 1970a. Infrared absorption spectrum of water adsorbed on alpha-helical synthetic polypeptides. *Nature.* 227:1358–1360.

Malcolm, B. R. 1970b. Surface chemistry of poly (beta-benzyl-L-aspartate). *Biopolymers.* 9:911–922.

Marsh, R. E., R. B. Corey, and L. Pauling. 1955. An investigation of the structure of silk fibroin. *Biochem. Biophys. Acta.* 16:1–35.

Maste, M. C. L., W. Norde, and A. Visser. 1997. Adsorption-induced conformational changes in the serine proteinase savinase: a tryptophan fluorescence and circular dichroism study. *J. Colloid Interface Sci.* 196:224–230.

Matsuno, K., R. V. Lewis, and C. R. Middaugh. 1991. The interaction of gamma-crystallins with model surfaces. *Arch. Biochem. Biophys.* 291: 349–355.

McGrath, K., and D. Kaplan. 1997. Protein-based materials. *In* Bioengineering of Materials. D. Kaplan, editor. Birkhäuser, Boston. 429.

Mita, K., S. Ichimura, and T. C. James. 1994. Highly repetitive structure and its organization of silk fibroin gene. *J. Mol. Evol.* 38:583–592.

Narsimhan, G., and F. Uraizee. 1992. Kinetics of adsorption of globular proteins at an air-water interface. *Biotechnol. Prog.* 8:187–196.

Norde, W., and T. Zoungrana. 1998. Surface-induced changes in the structure and activity of enzymes physically immobilized at solid/liquid interfaces. *Biotechnol. Appl. Biochem.* 28:133–143.

Peak Fit. 1997. ImageStream Graphics and Presentation Filters. Peak Fit, Chicago, IL.

Rippon, W., and A. Walton. 1971. Optical properties of the polyglycine II helix. *Biopolymers.* 10:1207–1212.

Rippon, W. B., and A. G. Walton. 1972. Spectroscopic characterization of poly(Ala-Gly-Gly). *J. Am. Chem. Soc.* 94:4319–4324.

Ronish, E. W., and S. Krimm. 1972. Theoretical calculation of the circular dichroism of unordered polypeptide chains. *Biopolymers.* 11: 1919–1928.

Ronish, E. W., and S. Krimm. 1974. The calculated circular dichroism of polyproline II in the polarizability approximation. *Biopolymers.* 13: 1635–1651.

Rothwarf, D. M., V. G. Davenport, P.-T. Shi, J.-L. Peng, and H. A. Sheraga. 1996. Use of sequence-specific tri-block copolymers to determine the helix-forming tendencies of amino acids. *Biopolymers.* 39: 531–536.

Shah, N. K., M. Sharma, A. Kirkpatrick, J. A. Ramshaw, and B. Brodsky. 1997. Gly-Gly-containing triplets of low stability adjacent to a type III collagen epitope. *Biochemistry.* 36:5878–5883.

Simmons, A. H., C. A. Michal, and L. W. Jelinski. 1996. Molecular orientation and two-component nature of the crystalline fraction of spider dragline silk. *Science.* 271:84–87.

Smith, L. J., and D. C. Clark. 1992. Measurement of the secondary structure of adsorbed protein by circular dichroism. 1. Measurements of the helix content of adsorbed melittin. *Biochim. Biophys. Acta.* 1121: 111–118.

Stuart, B. 1997. Biological Applications of Infrared Spectroscopy. John Wiley and Sons, Cambridge.

Takahashi, Y. 1994. Crystal structure of silk of *Bombyx mori. In* Silk Polymers: Materials Science and Biotechnology. D. Kaplan, W. W. Adams, B. Farmer, and C. Viney, editors. American Chemical Society, Washington, DC. 168–175.

Thiel, B. L., K. B. Guess, and C. Viney. 1997. Non-periodic lattice crystals in the hierarchical microstructure of spider (major ampullate) silk. *Biopolymers.* 41:703–719.

Tiffany, M. L., and S. Krimm. 1972. Effect of temperature on the circular dichroism spectra of polypeptides in the extended state. *Biopolymers.* 11:2309–2316.

Valluzzi, R., and S. P. Gido. 1997. The crystal structure of *Bombyx mori* silk fibroin at the air-water interface. *Biopolymers.* 42:705–717.

Valluzzi, R., S. P. Gido, W. Muller, and D. Kaplan. 1999b. Orientation of silk III at the air-water interface. *Int. J. Biol. Macromol.* 24:237–242.

Valluzzi, R., S. Gido, W. Zhang, W. Muller, and D. Kaplan. 1996. A trigonal crystal structure of *B. mori* silk incorporating a threefold helical conformation found at the air-water interface. *Macromolecules.* 29: 8606–8614.

Valluzzi, R., S. J. He, S. P. Gido, and D. Kaplan. 1999a. *B. mori* silk fibroin liquid crystallinity at aqueous fibroin-organic solvent interfaces. *Int. J. Biol. Macromol.* 24:227–236.

Van Beek, J. D., J. Kummerlen, F. Vollrath, and B. H. Meier. 1999. Supercontracted spider dragline silk: a solid-state NMR study of the local structure. *Int. J. Biol. Macromol.* 24:173–178.

Winkler, S., S. Szela, P. Avtges, R. Valluzzi, D. Kirschner, and D. L. Kaplan. 1999. Designing recombinant spider silk proteins to control assembly. *Int. J. Biol. Macromol.* 24:265–270.

Wu, H., Y. Fan, J. Sheng, and S. F. Sui. 1993. Induction of changes in the secondary structure of globular proteins by a hydrophobic surface. *Eur. Biophys. J.* 22:201–205.

Yoshimizu, H., and T. Asakura. 1990. The structure of *Bombyx mori* silk fibroin membrane swollen by water studied with ESR, C-NMR, and FT-IR spectroscopies. *J. Appl. Polym. Sci.* 40:1745–1756.